

EARLY ONLINE RELEASE

This is a PDF of a manuscript that has been peer-reviewed and accepted for publication. As the article has not yet been formatted, copy edited or proofread, the final published version may be different from the early online release.

This pre-publication manuscript may be downloaded, distributed and used under the provisions of the Creative Commons Attribution 4.0 International (CC BY 4.0) license. It may be cited using the DOI below.

The DOI for this manuscript is

DOI:10.2151/jmsj.2024-018

J-STAGE Advance published date: February 27th, 2024

The final manuscript after publication will replace the preliminary version at the above DOI once it is available.

1 **Revisiting Koba's relationship to improve minimum sea-level**
2 **pressure estimates of western North Pacific tropical cyclones**

3

4

Masataka AIZAWA

5

Graduate School of Engineering Science, Akita University, Akita, Japan

6

Kosuke ITO*

7

Disaster Prevention Research Institute, Kyoto University, Uji, Japan

8

Typhoon Science and Technology Research Center, Yokohama National University,

9

Yokohama, Japan

10

Udai SHIMADA

11

Meteorological Research Institute, Japan Meteorological Agency, Tsukuba, Japan

12

13

Submitted to the *Journal of the Meteorological Society of Japan*

14

16 January, 2024

15

16

* Corresponding author: Kosuke Ito, *Kyoto University, Uji, Japan*

17

Email: ito.kosuke.2i@kyoto-u.ac.jp

18

Tel: +81-774-38-4159

19

Fax: +81-774-38-4158

20

Abstract

Currently, the Regional Specialized Meteorological Center Tokyo applies the satellite-based Dvorak technique using the relationship developed by Koba et al. (1990) for one of the important sources of tropical cyclone (TC) intensity analysis. To improve TC intensity analysis, we revisited Koba's relationship used for estimating the minimum sea level pressure (MSLP) considering case selection, aircraft data treatment, current intensity (CI) numbers, and additional explanatory variables. The root mean squared difference (RMSD) of the MSLP between the aircraft data and the concurrent estimates based on the original formula of Koba et al. (1990) is approximately 13.0 hPa. The RMSD reduced by 28% to 9.3 hPa in the revised regression model that used CI numbers analyzed through modern methods and additional explanatory parameters (development rate, size, latitude, and environmental pressure) with careful treatment of the aircraft data. The signs of the coefficients in the proposed model suggest that the actual MSLP change lags the change in the corresponding CI number. The large TC at high latitudes with lower environmental pressure has a low MSLP for a given CI number. Cross-validation results supported the superiority of the proposed model. The current approach is simple but substantially improves the quality of the TC intensity analysis, leading to improved TC forecasts through TC bogus, wave models, storm surge models, and forecast verification.

Keywords: tropical cyclones; Dvorak technique; historical dataset

42 **1. Introduction**

43 The estimation of tropical cyclone (TC) intensity parameters, such as the
44 maximum sustained 10-meter wind speed (V_{max}) and minimum sea-level pressure
45 (MSLP), is essential for disaster prevention and mitigation. This is related to the severity of
46 the disaster, preparedness of the people, and decision-making by the government.
47 Currently, the Regional Specialized Meteorological Center (RSMC) Tokyo - Typhoon
48 Center in JMA, issuing TC advisories in the Western North Pacific (WNP) within the
49 framework of the World Weather Watch program of the World Meteorological Organization,
50 applies the satellite-based Dvorak method (Dvorak 1975, 1984) using tables developed by
51 Koba et al. (1990; hereafter K90)¹ as one of the important sources of TC intensity analysis,
52 particularly for TCs in the open ocean. Satellite analysts at JMA examine satellite images
53 and utilize the Dvorak Technique to derive a tropical (T) number with situational
54 constraints (Dvorak 1984). A current intensity (CI) number is determined considering the T
55 number and TC stages (Lushine 1977). The tables in K90 convert the CI number to MSLP
56 and V_{max} . The K90 tables were constructed with the match-up of satellite imagery and
57 JMA best track² datasets from 1981 to 1986, when aircraft observation missions flown by

¹ K90 was written in Japanese, but the main content was translated into an English version, Koba, H., T. Hagiwara, S. Osano, and S. Akashi, 1991a: Relationships between CI Number and minimum sea level pressure/maximum wind speed of tropical cyclones. *Geophysical Magazine*, **44**, 15-25.

² Note that RSMC Tokyo was established in 1989 after the study period of 1981–1986. While the archived best track data is currently managed by RSMC Tokyo, we use the term JMA best track, which is typically referred to as the RSMC Tokyo best track.

58 the U.S. Air Force in support of the Joint Typhoon Warning Center (JTWC) were routinely
59 conducted.

60 The sample mean of the estimated TC intensity in each CI number category based
61 on K90 was shown to be reasonable (Kitabatake et al. 2018; Knaff and Zehr 2007).
62 However, the individual TC intensities contained errors in some cases. For example, Ito et
63 al. (2018) reported that the difference in the MSLP was -10 hPa (935 and 925 hPa) at 06
64 UTC on October 21, 2017, and +15 hPa at 00 UTC on October 22 (915 and 930 hPa) for
65 TC Lan (2017) between the K90-based estimations and aircraft dropsonde observations in
66 Tropical cyclones-Pacific Asian Research Campaign for Improvement of Intensity
67 estimations/forecasts (T-PARCII), which penetrated the eyewall of the intense TC with a
68 Gulfstream II jet. The data assimilation of T-PARCII dropsonde observations in Ito et al.
69 (2018) showed that the intensity forecast errors generally decreased when the real-time
70 analysis was used as a baseline; however, they increased when the best track was used.
71 In that case, the dropsonde-based estimate of the MSLP was closer to the real-time
72 analysis, suggesting that the intensity forecast skill could not be correctly evaluated owing
73 to the uncertainties in the intensity estimation. In fact, the estimated root mean squared
74 difference (RMSD) of the individual MSLP data from the regression line in K90 is similar to
75 the 24-h forecast errors, as shown in Section 2. Accurate TC intensity analysis is also
76 important for forecasts because it is used as bogus observations in data assimilation and
77 inputs for wave and storm surge forecasts. Furthermore, improved quality contributes to

78 the evaluation of the impacts of climate change on TCs (Kawabata et al. 2023).

79 The errors in individual TC intensity analyses partly stem from the difficulty in
80 specifying CI numbers (Bai et al. 2023; Bai et al. 2019; Nakazawa and Hoshino 2009).
81 Although the difference in the estimated CI numbers among operational centers is
82 generally small (Bai et al. 2023), the value is sometimes dubious, for example, because
83 upper-level clouds mask the structure (Yamada et al. 2021). In addition to the specification
84 of the CI number, the residual from the regression line in K90 imposes errors in individual
85 TC intensity estimations, even with the correct CI number. When the K90 table was
86 constructed, an individual MSLP observed by aircraft from 1981 to 1986 often deviated
87 significantly from the regression curve, as shown in Fig. 1. The final TC intensity estimate
88 is assigned based on the CI number in the current K90 procedure, whereas the actual TC
89 intensity may depend on parameters other than the wrong assignment of CI numbers. The
90 residual can be ascribed to various reasons such as measurement errors, dependency on
91 latitude and size, differences in environmental pressure, improper treatment of
92 observations, and incorrect specifications of CI numbers when constructing the regression.
93 Therefore, it is necessary to determine whether there is any potential to decrease these
94 errors.

95 This paper briefly reexamines the procedure of K90, and investigated the potential
96 for improvements across four aspects: First, match-up cases should be selected carefully.
97 For example, the K90 formula was constructed using the JMA best-track data and not

98 necessarily aided by aircraft-based observations. Second, data processing from aircraft
99 observations of TC intensity should be carefully checked. Third, the CI numbers can be
100 better specified in a modern manner (Kitabatake et al. 2018). The use of reanalyzed CI
101 numbers for TCs during 1981–1986 by Tokuno et al. (2009) reflects some updated
102 procedures for the Dvorak technique. Finally, the explanatory variables, in addition to the
103 CI numbers, can be considered to construct a model deriving more robust TC intensity.
104 The last item is strongly motivated by Knaff and Zehr (2007) who developed a wind-
105 pressure relationship by binning individual data according to latitude, TC size, storm
106 motion, and environmental pressure, followed by a further update by Courtney and Knaff
107 (2009). They successfully reduced the scatter of the MSLP between observations and
108 estimations for a given V_{max} . In this study, we consider the procedures outlined to
109 develop a new model for estimating the MSLP in the western North Pacific as a function of
110 latitude, TC size, environmental pressure, and CI number using data from 1981 to 1986.

111 We focused on the estimate of the MSLP rather than V_{max} or the wind-pressure
112 relationship, although we recognize that V_{max} is important for disasters. This is because
113 in the 1980s, the MSLP was reasonably measured by flight-level altitudes, which are good
114 proxies for the MSLP, or dropsondes. In contrast, V_{max} was crudely observed from on-
115 board observations of the sea surface state and flight-level wind measurements reduced to
116 the surface. Those V_{max} observations were limited to the regions of the flight path. The
117 final analysis of V_{max} by JMA was largely due to the MSLP using an approximate form of

118 cyclostrophic wind balance (Atkinson and Holliday 1977; Takahashi 1952). Therefore, it is
119 reasonable to focus on the development of a reliable model for MSLP estimation in the
120 WNP as a first step toward estimating the TC Vmax. Our perspective on Vmax estimation
121 is provided in the concluding remarks.

122 The remainder of this paper is organized as follows: Section 2 briefly describes the
123 background and methodology of the K90. In Section 3, we evaluate the selected cases,
124 treatment of aircraft-based observations, use of reanalyzed CI numbers, and additional
125 explanatory variables. A new model for estimating the MSLP is proposed and evaluated in
126 Section 4, and we apply further tests in Section 5. The concluding remarks are presented
127 in Section 6. This study aids in more accurately estimating the TC MSLP, which should
128 lead to more reliable TC forecasts and verifications, as well as a better evaluation of the
129 impact of climate change on TCs.

130

131 **2. Revisiting K90**

132 The objective of K90 was to compare the relationship between CI numbers and TC
133 intensity (MSLP and Vmax) analyzed by the JMA, although the tables in Dvorak (1975)
134 and Dvorak (1984) were available. We briefly review the processes in terms of case
135 selection, treatment of aircraft data, CI numbers, and regression equation.

136

137 **2.1 Case selection**

138 The intensity estimates of TCs by the JMA relied on aircraft reconnaissance by the U.S.
139 Air Force and JTWC until 1987. The JMA started to routinely derive CI numbers in March
140 1987 to conduct a Dvorak analysis. They used 50 TCs whose lifetime minimum for the
141 MSLP was 950 hPa or less in the JMA best track data from 1981 to 1986, except for the
142 seemingly incorrect specification of two TCs (TC Doyle (1984) and TC Judy (1982) as
143 shown below). Although it is unclear why they did not employ TCs whose lifetime MSLP
144 was higher than 950 hPa, it effectively alleviated excessive adjustment to samples for
145 weak TCs, which degraded the intensity estimation of very strong TCs (Knaff and Zehr
146 2007). They used 12-hourly best track data (00 and 12 UTC) instead of the 6-hourly best
147 track. Although 50 TCs were flown by reconnaissance aircraft at least 10 times,
148 approximately 40% of the best track records were not aided by the aircraft observations
149 within 3 h from the analysis time. This could be a source of uncertainty in the K90
150 derivations. Unfortunately, the individual records used to construct the K90 table are
151 missing. However, we can discuss some of the basic properties of K90 using its texts,
152 tables, and figures.

153 Based on the text, 50 TCs were allegedly analyzed. However, their list of TCs
154 (Table 2 of K90) contained only 48 TCs and exhibited some inconsistencies as follows.

- 155 ● TC Doyle (1984), whose lifetime minimum MSLP was 940 hPa, was not listed,
156 although aircraft observations were available.
- 157 ● The lifetime minimum of the MSLP of TC Judy (1982) in the table was 955

158 hPa.

- 159 ● TC Dinah (1984) was misspelled as TC Dainah (1984).
- 160 ● An incorrect identification number was assigned to the TCs Agnes (1981),
161 Clara (1981), Elsie (1981), Gay (1981), Carmen (1986), Forrest (1986) and
162 Joe (1986) in their Table 2. For example, TC Agnes was the 18th TC in 1981.
163 This was recorded as the 20th TC in the table. The wrong identification
164 numbers caused two TCs (Irma (1981) and Kim (1986)) to be missing in Table
165 2 of K90, although their lifetime MSLPs were lower than 950 hPa. This may
166 explain why only 48 TCs are listed in this table, instead of 50. Although these
167 two TCs are not shown in Table 2 of K90, their tracks are on the map (Fig. 1 of
168 K90); thus, it can be assumed that they were used in the analysis of K90.

169 In K90, the reported total number of samples was 855. However, our count of the
170 number of samples for the 12-hourly best track was 811 for the 50 TCs. Even when we
171 add Doyle (1984) to the count, the number is 822. The reasons for these inconsistencies
172 are unclear. Nevertheless, the histograms of the MSLP in the K90 record and our count for
173 the 51 TCs were similar (Fig. 2). These factors were unlikely to affect the results and
174 conclusions hereafter.

175

176 2.2 Treatment of aircraft data

177 K90 used the best track data for constructing the regression equation. The

178 correlation coefficient between the best track MSLP and aircraft-based MSLP was as
179 much as 0.99 when those aircraft data were available. Therefore, the best track data
180 heavily relied on the aircraft-based observations if available. During that period,
181 dropsondes and the converted MSLP from aircraft altitude were used. For the conversion
182 from the aircraft altitude, the conversion formula (Watanabe's equation) was used to obtain
183 the MSLP on those days in the JMA (Kitabatake et al. 2018).

$$P_c = 634 + 0.1194x \quad (1)$$

184 where x represents the aircraft altitude at 700 hPa in meters.

185 This study mainly focused on the MSLP estimation. However, one may be
186 interested in the Vmax estimation. Based on an interview with a person who performed the
187 TC intensity analysis on those days, the Vmax predominantly relied the conversion from
188 MSLP, although the surface wind estimation and flight-level winds were frequently
189 reported (Y. Nyomura, 2022, personal communication, October 31, 2022). We calculated
190 the correlation coefficients between the best track Vmax and possible sources for the
191 cases in which both the surface wind estimation and flight level winds were available. The
192 correlation coefficient was 0.70 between the best track Vmax and surface wind estimation
193 and 0.84 between the best track Vmax and flight level winds. In contrast, the correlation
194 coefficient was 0.97 between best track Vmax and Vmax converted from best track MSLP,
195 following $V_{\max} = 6.0 \times \sqrt{1010 - \text{MSLP}}$ (Takahashi 1952)³. This strongly suggests that the best

³ Several formulae were also used to convert from the MSLP to the Vmax on those days (Nyomura, 2022,

196 track Vmax depended on the best track MSLP rather than the aircraft-based information
 197 on sea surface wind estimates and flight-level winds on those days.

198

199 2.3 CI numbers

200 A CI number in K90 was estimated from an enhanced infrared satellite imagery
 201 according to the Dvorak technique, while a visible satellite imagery was also referenced
 202 during the daytime. Four skillful analysts have worked on this project. However, it was
 203 likely that one analyst determined the CI number, except for difficult cases in which the
 204 decision was made by two analysts. The CI number for a TC that decayed over land was
 205 determined by the algorithm in Koba et al. (1991b).

206

207 2.4 Regression equation

208 K90 proposed a quadratic function for the MSLP and Vmax using the CI number
 209 as the explanatory variable. The regression models derived⁴ for all samples were

$$P_c = -1.53CI^2 - 3.03CI + 1010.01 \quad (2)$$

$$V_{\max} = 0.09CI^2 + 13.49CI + 8.38 \quad (3)$$

210 where P_c is the MSLP in hPa, and V_{\max} is the 10-minute averaged wind in knot. The
 211 outputs were tabulated for operational purposes. K90 also derived models for the

personal communication, October 31, 2022).

⁴ Eq. (2) is taken from Fig. 2a of K90. The equation on page 66 of K90 is incorrect.

212 developing and decaying cases. The MSLP was higher (lower) for CI numbers smaller
213 (larger) than 4.0 in developing cases, while K90 recommends the use of Eq. (2) that does
214 not consider the development rate. They mentioned an overestimation in Dvorak (1984) for
215 the intensity of strong cyclones, which is consistent with recent surveys (Knaff and Zehr
216 2007).

217 The RMSD of the residuals between individual data and this regression equation
218 was 12.99 hPa (including the rounding error for the best track data to 5-hPa) from Fig. 2 of
219 K90 (Fig. 1). This implies that even if a CI number is appropriately assigned, each MSLP
220 estimation significantly deviates from the truth. Comparing this with the root mean squared
221 errors of recent TC intensity forecasts by JMA (11.9 and 18.1 hPa at the forecast times of
222 24 and 72 h from 2017 to 2021, respectively, based on RSMC Tokyo annual reports), a
223 large error in the MSLP estimate could degrade the subsequent TC intensity forecasts
224 through data assimilation, as well as hindering a correct evaluation of the forecast skill
225 especially for an individual case.

226

227 **3. Improvement potentials**

228 Based on the K90 procedure reviewed, we considered the selected cases, aircraft data
229 treatment, CI numbers, and additional explanatory variables for a better TC intensity
230 analysis model.

231

232 3.1 Case selection

233 The best-track data were used to create the K90 table regardless of the aircraft
234 observations around the specified time. If there were aircraft observations around the time
235 of analysis, the MSLP in the best track data was expected to be more reliable. However, if
236 there were no supportive aircraft observations around the time of analysis, the MSLP on
237 the best track was less reliable. It is reasonable to construct a regression model using only
238 aircraft observations from around the time of analysis including TC Doyle (1984), whose
239 lifetime MSLP was 940 hPa. In addition, we used 6-hourly aircraft data instead of the 12-
240 hourly data used in K90.

241

242 3.2 Treatment of aircraft data

243 We checked the aircraft data from 1981 to 1986, as in K90. Aircraft data from 1981
244 to 1985 were obtained from the JTWC annual reports while those from 1986 were
245 provided by the JTWC. When a record was dubious, based on our basic checks, we also
246 referred to the JMA Geophysical Review, which describes JTWC aircraft data since 1951.
247 The basic checks were as follows.

- 248 ● Some records show that the 700 hPa height was observed reportedly at the
249 vertical level of 1,500 ft. Of course, the 700 hPa height cannot be directly
250 observed from 1,500 ft. After checking the consistency in the succeeding
251 aircraft reconnaissance, we assumed that this was due to a written mistake in

252 the vertical level, which should have been 700 hPa; we used the 700 hPa
 253 height for the MSLP estimation.

254 ● If one aircraft-based MSLP ($MSLP_a$) was spiky, the $MSLP_a$ was not used. This
 255 condition is expressed as follows:

$$|MSLP_{\text{before}} - MSLP_a| > 30 \text{ hPa},$$

$$|MSLP_{\text{after}} - MSLP_a| > 30 \text{ hPa},$$

$$(MSLP_{\text{before}} - MSLP_a)(MSLP_{\text{after}} - MSLP_a) < 0,$$

256 where $MSLP_{\text{before}}$ and $MSLP_{\text{after}}$ are respectively the aircraft-based MSLPs
 257 obtained within 6 h before and after the observation time of $MSLP_a$.

258 ● If the 700 hPa height was greater than 3,200 m, the data were not used.
 259 ● When both dropsondes and flight altitudes were available for MSLP estimation,
 260 the data were not used if the two estimates deviated by more than 10 hPa.

261

262 To convert an aircraft altitude to an MSLP, we employed the following formula from
 263 Jordan (1958):

$$P_c = 645 + 0.0115x \quad (4)$$

264 We used this formula from Jordan (1958) instead of Eq. (1) because Watanabe's formula
 265 incurs an estimation bias. A comparison between the dropsonde-derived MSLP and the
 266 MSLP converted from aircraft altitude using Eq. (1) shows that the altitude-derived MSLP
 267 tended to have negative bias for very strong TCs while it tended to have positive bias for

268 moderate-to-weak TCs (Fig. 3a). Thus, the MSLP estimated from the flight altitudes
269 according to Eq. (1) may have caused a bias. The optimal linear regression between the
270 altitude and dropsonde data was as follows:

$$P_c = 646 + 0.01145x \quad (5)$$

271 This is significantly closer to the relationships in Eq. (4) as in Jordan (1958); therefore, the
272 use of Jordan's formula enhances the consistency between dropsonde-derived MSLPs
273 and MSLPs converted from altitude. Dropsondes provide direct observation of the MSLP
274 and serve as a reference. They were used in our new TC intensity analytical model.
275 whereas we admit that the dropsonde-derived MSLP sometimes deviates from the true
276 MSLP by a few hPa. For example, it is difficult to accurately detect the center of a weak
277 TC without a clear eye. In addition, the location of an observation can be slightly away
278 from the surface center horizontally and vertically. The National Hurricane Center corrects
279 the MSLP according to the observed splash wind. However, we are unsure that this type of
280 correction was not applied on those days. The actual splash wind was at least not
281 accurately observed at that time.

282

283 *3.3 CI numbers*

284 Although the original CI number records used by K90 are missing, the reanalyzed
285 CI numbers of Tokuno et al. (2009) were available for TCs from 1981 to 1986. This version

286 treats CI numbers as follows:

- 287 ● The largest T number in the lifetime of the TC was determined first. Subsequently,
- 288 a Dvorak analysis was conducted forward and backward in time, which worked
- 289 better for estimating the intensity of a rapidly evolving TC. We note that this is not
- 290 in the JMA operational real-time analysis procedure.
- 291 ● The 6-hourly analysis was conducted with 3-hourly animated images.
- 292 ● The square-lattice projection was used. This projection is less affected by image
- 293 distortion.

294 Kitabatake et al. (2018) stated that the quality of the CI numbers is presumably better in
 295 terms of the accuracy and homogeneity.

296

297 3.4 Additional explanatory variables

298 Knaff and Zehr (2007) explained that the TC tangential wind speed, v , and the TC
 299 MSLP, P_c , are related through the gradient wind balance as follows:

$$P_c = -\int_0^R \rho \left(\frac{v^2}{r} + fv \right) dr + P_{env} \quad (6)$$

300 where ρ is the density, r is the distance from the center, R is the radius of interest, f is the
 301 Coriolis parameter, and P_{env} is the environmental pressure. This equation states that the
 302 MSLP is not solely a function of tangential wind and thus supports the idea of using the TC
 303 size, Coriolis parameter (or latitude), and environmental pressure for the pressure-wind

304 relationship (Bai et al. 2023; Courtney and Knaff 2009; Knaff and Zehr 2007). Under the
305 framework of K90, which considers the relationship between the MSLP and CI number
306 (not the relationship between the MSLP and V_{max}), it is worth investigating how the MSLP
307 is related to parameters other than the CI numbers. The CI number is determined by the
308 cloud status around the TC center and reflects its vorticity, convection, core temperature,
309 and the effect of environmental vertical wind shear (Velden et al. 2006). It relies less on TC
310 size, latitude, and environmental pressure. Therefore, it is reasonable to include the size,
311 latitude, and environmental pressure as explanatory variables to explain the variability in
312 MSLPs. In addition to these variables, K90 showed that the relationship between the
313 MSLP and CI numbers also depended on the development rate of a TC. It may be
314 valuable to include the development rate as an additional explanatory variable.

315 Our regression model is similar to those developed by Knaff and Zehr (2007) and
316 others with several differences. Previous models have considered the translation speed of
317 a TC. However, we did not consider the TC translation speed to adjust the wind speed
318 because the regression model in our study did not explicitly consider the wind. We also
319 propose a model in which the product of latitude and TC size is treated as an explanatory
320 variable, in addition to one that considers latitude and TC size as two independent
321 variables. This is because Eq. (6) indicates that the product is more relevant to the MSLP.

322

323 **4. MSLP model**

324 *4.1 Regression equations and data treatment*

325 Based on these considerations, we tested nine equations, as summarized in Table
326 1. The original equation proposed by K90 is referred to as CTRL. The other equations
327 employ Jordan's conversion formula from aircraft altitude to MSLP, while CTRL employs
328 Watanabe's formula. The JORDAN experiment was performed to show the dependence of
329 the skill to the different conversion formulae. The CIOPTIM equation is the quadratic
330 regression expression optimized for the CI numbers in Tokuno et al. (2009). DEVELOP,
331 LAT, SIZE, and PENV are similar to CIOPTIM but they each add the development rate,
332 latitude, size, and environmental pressure as an explanatory variable in the regression
333 expressions. The TEST1 equation considers the CI number, development rate, latitude,
334 size, and environmental pressure as explanatory variables. The TEST2 equation is similar
335 to the TEST1 equation, but employs the product of latitude and size as one explanatory
336 variable instead of independently employing latitude and size as two explanatory variables.
337 Through this series of equations, we aimed to clarify the improvement of the MSLP
338 estimation using updated CI numbers, updated altitude-MSLP relationships, and additional
339 explanatory variables discussed in Section 3.4 on the MSLP estimation against the
340 calibrated aircraft-based MSLP observations (dropsonde or flight-level altitude).

341 We used 6-hourly aircraft-based MSLP observations for 51 TCs whose lifetime
342 MSLP was 950 hPa or lower from 1981 to 1986 except for TC Judy (1982). The sampled
343 TCs were presumably the same as in K90, except TC Doyle (1984) was added in the

344 current analysis.

345 We employed CI numbers from Tokuno et al. (2009). In the operational procedure
346 of the JMA, the maximum change in T numbers should be equal to or smaller than ± 1.0 in
347 6 h, ± 1.5 in 12 h, ± 2.0 in 18 h, and ± 2.5 in 24 h (Kitabatake et al. 2018). Tokuno et al.
348 (2009) constructed two versions of CI numbers with and without the limitation. We show
349 the results without this limitation because the RMSD was slightly smaller (approximately
350 0.4 hPa in TEST1). After applying the basic quality controls mentioned in Section 3.2, the
351 6-hourly MSLP was calculated from dropsondes or flight-level altitudes only when aircraft
352 data were available within 3 h of the analysis time. When both dropsonde- and altitude-
353 based MSLPs were available (444 cases), their mean was employed as the observed
354 MSLP because the errors in dropsonde- and altitude-based MSLPs likely cancel out⁵.
355 When multiple aircraft missions were conducted within 3 h of the analysis time, only one
356 mission nearest to the analysis time was used. If the TC center was located within 0.1°
357 from the land in the last 12 h, the data were not used. We tested Eqs. (1) and (4) for the
358 conversion of aircraft altitude to the MSLP. In total, 877 records were used to construct the
359 regression models.

360 Latitude, used as the explanatory variable, was obtained from the JMA best track.
361 The change in the CI number (δCI_{24}) is represented by the difference between the current

⁵ The RMSD of TEST1 in Table 1 was 9.60 hPa by employing a dropsonde observation for the MSLP for these 444 cases while the corresponding RMSD was 9.55 hPa by employing the average of a dropsonde observation and altitude-inferred estimate with the same samples.

362 CI number and the CI number 24 h prior. If the CI number 24 h prior was not available, the
363 change in the CI number was set to zero. The radius of the 30-kt wind (R30) in the JMA
364 best track from 1981 to 1986 was available and appears to fit the operational purpose. The
365 official R30 was basically determined based on reports from ships and buoys, satellite
366 observations, and clouds from those days but MSLP might be preferred (JMA 1990). Thus,
367 the use of the best track R30 as an explanatory variable is not appropriate to derive a
368 regression equation. Another potential issue is that the characteristics of the official R30
369 estimates have substantially changed over the last several decades. The correlation
370 coefficient between R30 and MSLP was -0.61 from 1981 to 1986, while it was -0.40 from
371 2016 to 2021. This implies that an optimized model with R30 on those days does not show
372 the envisaged skill in operational use to date. Therefore, we employed a radius for the
373 azimuthal-mean tangential velocity of 20 kt in ERA5 (Hersbach et al. 2020) for the TC size
374 ($R_{20_{\text{ERA}}}$) because the size of a TC in ERA5 is not directly affected by the MSLP. We
375 determined the TC center in ERA5 as the location of the MSLP minimum after applying the
376 smoothing of 3x3 grids and calculated the azimuthal-mean tangential velocity about the TC
377 center. When the maximum azimuthal-mean tangential velocity in ERA5 was less than 20
378 kt or the TC size was smaller than 100 km, the TC size was set to 100 km. Environmental
379 pressure was calculated as the average within the ring between $R_{20_{\text{ERA}}}+100$ km and
380 $R_{20_{\text{ERA}}}+300$ km. In Section 5.2, we show the results of additional experiments that
381 employed the R30 in the JMA best track, Japanese 55-year Reanalysis (JRA55;

382 Kobayashi et al. 2015), or the radius of the outermost closed isobar (ROCI).

383

384 *4.2 Results*

385 The coefficients of each regression model are summarized in Table 2, and their
386 RMSDs with respect to the aircraft data are shown in Table 3 and Fig. 4. Table 3 lists two
387 RMSDs to quantify the adverse effect of the rounding of aircraft-based MSLPs and
388 regression model outputs to 5-hPa on the intensity estimation. The rounding to the nearest
389 5-hPa was applied to be fair with the RMSD of the MSLP from Fig. 2 in K90 (12.99 hPa).
390 The RMSD of CTRL was 12.54 hPa without rounding to the 5-hPa bin. This is smaller than
391 the estimated RMSD of K90, as discussed in Section 2. The differences arise from the
392 different case selections and CI numbers, as well as the rounding. Out of these factors, the
393 rounding to the 5-hPa bin explains the increase of 0.08 hPa (Table 3). Assuming that the
394 CI numbers in Tokuno et al. (2009) are closer to the current JMA operational Dvorak
395 analysis than K90, the operational Dvorak analysis with the K90 table does not degrade
396 the quality of the TC intensity. JORDAN yields an RMSD of 12.29 hPa, which is smaller
397 than those in CTRL. This is due to the better consistency between the dropsonde-based
398 MSLP and MSLP converted from aircraft altitude using Jordan (1958). CIOPTIM yields an
399 RMSD of 11.86 hPa, which is lower than those of CTRL and JORDAN. This presumably
400 reflects the smaller scatter from the better specification of the CI numbers in Tokuno et al.
401 (2009).

402 By adding either the development rate, latitude, TC size, or environmental
403 pressure as an explanatory variable (DEVELOP, LAT, SIZE, PENV), the RMSDs
404 decreased by 0.48–1.40 hPa relative to CIOPTIM. This suggests that the addition of
405 these parameters to the CI numbers partly explains the scatter of the MSLP, as in the
406 addition of these parameters to Vmax in Knaff and Zehr (2007). In particular, a significant
407 improvement was achieved when the latitude or size was added as an explanatory
408 variable.

409 TEST1 considered all additional four parameters as explanatory variables, with
410 size and latitude as independent variables. The RMSD of TEST1 was 9.34 hPa, which
411 was 25.5% lower than that of CTRL. This suggests that the optimization with CI numbers
412 through modern methods and the consideration of additional parameters can
413 substantially improve the quality of the estimated MSLP for a better match to aircraft-
414 based observations that use the well-calibrated altitude-MSLP relationship.

415 The coefficients for size and latitude had negative signs in the regression equation
416 of TEST1 (Table 2), indicating that a lower MSLP was calculated for a large TC at higher
417 latitudes for a given CI number. This is reasonable because the CI number is relevant to
418 the structure around the TC center. The impact of size and latitude on the MSLP in Eq.
419 (6) persists over a broad area of the environment. The development rate term had a
420 positive sign. This implies that the weakening (intensifying) TC should be stronger
421 (weaker) for a given CI number. Thus, the change in the actual TC intensity lags behind

422 the CI-number change.

423 Fig. 5 shows the relationship between the aircraft-derived MSLP and the modeled
424 MSLP in CTRL and TEST1. A better fit was evident for all categories in the TEST1 model.
425 Cases with large analysis errors substantially decreased in TEST1 (Table 3 and Fig. 5).
426 The number of cases with a deviation of more than 25 hPa was 43 in CTRL, while it was
427 only 7 cases in TEST1. The regression model of TEST1 was stable because the busted
428 estimate was much less likely to occur. It is also notable that no models reasonably
429 reproduce the intensity of a TC with an MSLP < 900 hPa. This is an issue in intensity
430 analysis to be solved. One potential issue might be a specification of cloud patterns for a
431 CI number of 8.0. The CI number in K90 and Tokuno et al. (2009) was 7.5 at most; the
432 Dvorak-based TC MSLP could not be substantially lower than 900 hPa. Although the
433 number of the relevant samples is not large, this issue should be revisited in the future.

434 The large error cases in TEST1 include three samples from TC Forrest (1983). For
435 example, the recorded T and CI numbers for TC Forrest (1983) were 5.5 and 6.0,
436 respectively, yielding 936 hPa in TEST1 at 12 UTC on September 23, 1983 while the
437 dropsonde observation indicated 902 hPa. This is possibly because of the low resolution
438 of the satellite that was unable to capture a small TC eye. Aircraft reconnaissance
439 reported a small circular eye with a diameter of 6 miles. In contrast, Tokuno et al. (2009)
440 reported a ragged eye, which indicates a ragged eyewall or an indistinct eye, for this CI
441 number from a satellite image captured at that time. If the satellite images were of high

442 resolution, as in current satellites, the CI number would be higher. In another case of TC
443 Kit (1981) at 00 UTC on December 19, the aircraft-based intensity was 975 hPa, which
444 was significantly weaker than the output of TEST1 (946 hPa). The CI number analyzed
445 by Tokuno et al. (2009) was 6.0 for this case, while the CI number analyzed by JTWC
446 was 4.5. In this case, the difficulty for CI number specification possibly affects the error.

447 TEST2 is the same as TEST1, except that the product of the size and latitude is
448 used as an explanatory variable instead of employing them independently as two
449 explanatory variables. The RMSD of TEST2 (9.32 hPa) is very similar to that of TEST1
450 (9.34 hPa). There is a strong correlation between the TC size and latitude, as TC
451 circulations generally expand as they move poleward. This could be a reason why the
452 results did not differ significantly.

453

454 **5. Discussion**

455 *5.1 Cross validation*

456 One may wonder whether the TEST1 and TEST2 models exhibits better skills
457 simply because they are explained by several parameters. To ensure the integrity of the
458 TEST1 and TEST2 models, K-fold cross-validation was applied. In the K-fold cross-
459 validation, one-year data from 1981 to 1986 were used for validation, whereas data from
460 the other five years were used to construct the regression equation. Table 4 presents the
461 RMSDs values. The TEST1 model exhibited 22.7% better skill compared with the CTRL

462 model. The TEST2 model performed slightly better than the TEST1 model. This is
463 presumably because the smaller number of explanatory variables in TEST2 can explain
464 the variability as much as TEST1.

465

466 *5.2 Dependency on the definitions of size and environmental pressure*

467 Here we tested the dependence of model performance on the choice of a TC size
468 and environmental pressure. As for the size, we tested a radius of the azimuthal-mean
469 tangential velocity of 20 kt (R20) and a radius of the outermost closed isobar (ROCI) in
470 JRA55 and ERA5 as well as R30 in the JMA best track. In the calculation of R20 and
471 ROCI, we first applied the smoothing by taking the average of 3×3 grids to suppress grid-
472 scale noises. A TC center was defined as the location exhibiting the MSLP in the
473 smoothed field. The procedure to calculate the ROCI and relevant environmental pressure
474 is as follows: (1) grid points are defined at 1 km radially and 0.5° azimuthally within 2000
475 km from the TC center. (2) An innermost radius is calculated for a given sea level pressure
476 (initially an MSLP rounded up to the next integer) in each radial leg from the center to 2000
477 km. (3) An isobar is regarded as closed if the differences in two detected radii between
478 neighboring radial legs are all smaller than the corresponding azimuthal distance. (4)
479 When an isobar is closed, we add 1 hPa for a sea level pressure of interest and resume
480 the process (2). If the isobar is not closed, the mean radius of the outermost closed isobar
481 is regarded as the ROCI. (5) Finally, the environmental pressure was defined as the sea

482 level pressure at ROCI plus 1 hPa. When R20 or ROCI was smaller than 100 km, the TC
483 size was set to 100 km. R30 in the JMA best track is the simple mean of the longest and
484 shortest radius of 30 kt winds. The set of experiments are summarized in Table 5.

485 Table 6 lists the derived equations and RMSDs for LAT, PENV, TEST1, and
486 TEST2. Generally, the difference in performance was not sensitive to the choice of the
487 reanalysis dataset; the RMSDs for R30 in the best track were similar to those with R20
488 based on the reanalysis. The comparison between experiments C, D, E, and F indicates
489 that the skill was not much sensitive to the ring radius for environmental pressure when
490 R30 in the best track is employed. Dataset A exhibited the good skill while ERA5 does not
491 take account for the MSLP through TC bogussing. The use of ROCI for the size and
492 environmental pressure slightly degraded the skill, except for PENV.

493

494 **6. Summary and concluding remarks**

495 The conversion table in Koba et al. (1990) from a CI number to a TC intensity
496 measure (V_{max} or MSLP) has been used by the JMA. Recent research has shown that
497 the overall quality of this table is acceptable as a mean value, and it has made the gigantic
498 contribution to operational analyses and forecasts. However, the RMSD of the individual
499 MSLP records with respect to the regression line was estimated to be as much as 13.0
500 hPa. Deriving a better model for improved intensity estimates is therefore desirable,
501 leading to better forecasts and verifications. To do so, we revisited the procedure in Koba

502 et al. (1990) and investigated the potential for improvements through case selection,
 503 aircraft data checks, the use of reanalyzed CI numbers, and adding explanatory
 504 parameters.

505 First, the case selection process was re-examined. The reference data were
 506 originally obtained from the 12-hourly JMA best track for a TC whose lifetime minimum
 507 MSLP was 950 hPa or less based on Koba et al. (1990). In this study, 6-hourly reference
 508 data were taken from the aircraft-based MSLP within 3 h of the TC intensity analysis only
 509 when aircraft-based observations were available. We noticed that the conversion formula
 510 from aircraft altitude to MSLP used in the JMA at that time caused biases. Correction of
 511 the conversion formula decreased the RMSDs. We used the CI numbers in Tokuno et al.
 512 (2009) obtained through a modern procedure. Re-optimization of the coefficients in the
 513 formula further decreased the RMSDs. In addition to these treatments, we considered
 514 additional explanatory variables (development rate, size, latitude, and environmental
 515 pressure) in the MSLP estimation model. We found that all of them contributed to
 516 decreasing the RMSDs, of which size and latitude were important.

517 When we consider all of these factors, the derived models achieved the RMSDs as
 518 small as 9.34 and 9.32 hPa in the model construction and 9.69 and 9.54 hPa K-fold cross
 519 validation in the following models (TEST1 and TEST2 in Table 2), respectively.

$$P_c = -2.17CI^2 + 5.43CI + 1.73\delta CI_{24} - 0.367\Phi - 0.0227R - 5.78 + P_{env} \quad (7)$$

520 or

$$P_c = -2.21CI^2 + 5.68CI + 1.39\delta CI_{24} - 0.00113\Phi R - 12.81 + P_{env}. \quad (8)$$

521 Compared to the CTRL, the residual with respect to aircraft observations decreased by
522 more than 25% in the model construction (Table 3) and 22% in the verification (Table 4). If
523 we compare with the original table in Koba et al. (1990) that had approximately the RMSD
524 of 13.0 hPa (Fig. 1), the RMSD reduced by more than 28% to 9.3 hPa in the optimization.
525 Based on these coefficients, a large TC at high latitudes with low environmental pressure
526 tended to have a low MSLP in the model for a given CI number. This also suggests that
527 the change in the actual TC intensity lagged the change in the CI number. Additional
528 information on the size and latitude may decrease the scatter of the MSLP data. This may
529 reflect that the CI number is relevant to the structure around the TC center, while the
530 MSLP is also dependent on the outer environment. We also showed that the results are
531 robust but there is some dependency on the definition of the size, environmental pressure,
532 and the dataset (Table 6). The new regression models can contribute directly to intensity
533 estimation, indirectly to forecasting, verifying forecasts, and monitoring the impacts of
534 climate change.

535 Note that the general relationship between the CI number and MSLP has possibly
536 changed over the last 40 years. This question should be revisited by further aircraft
537 missions in the WNP and by considering the physical understanding of CI numbers in the
538 future. Also, the full use of microwave images and automation contribute to further
539 improving the quality of CI numbers (Olander and Velden 2019; Oyama 2014). This is

540 another important topic for investigation.

541 In this study, we did not extensively discuss the Vmax estimation. Many studies
542 and operational centers consider the procedure in which a forecaster first estimates Vmax
543 and proceeds to the conversion to the MSLP through the wind-pressure relationship. The
544 Vmax in the best track data was predominantly due to conversion from the MSLP in the
545 WNP because of the difficulty in Vmax observations from 1981 to 1986 (see also
546 supplemental material). If we estimate the MSLP by converting the Vmax to the MSLP, it
547 suffers from the combined effect of the Vmax estimation and conversion errors. It is
548 scientifically sound to first develop a model for the MSLP as accurately as possible and
549 then derive Vmax because the MSLP reference is relatively reliable. The uncertainty of the
550 MSLP can be quantified as in this study. The development of a procedure to derive Vmax
551 is highly important for disaster prevention and mitigation. For this purpose, one possible
552 means is to convert the MSLP to the Vmax through the wind-pressure relationship based
553 on Knaff and Zehr (2007), which is relatively reliable with in situ and remotely sensed
554 observations in the Atlantic and eastern Pacific regions. Another possible method is to
555 synthesize various observations such as dense dropsonde observations near the TC
556 inner-core region (Yamada et al. 2021), ground-based Doppler radar (Shimada et al. 2016),
557 and synthetic aperture radar (Zhang et al. 2014) in the WNP, which is beyond the scope of
558 this study.

560 **Supplement**

561 The supplement shows the skill of regression models using the MSLP and Vmax in
562 the best track data as a reference value.

564

565

Data Availability Statement

566 The TC best-track data are available online on the RSMC Tokyo website

567 (<https://www.jma.go.jp/jma/jma-eng/jma-center/rsmc-hp-pub-eg/trackarchives.html>).

568 Dvorak reanalysis data were provided from RSMC Tokyo upon request. Aircraft

569 observation data from 1981 to 1985 were obtained from JTWC annual reports ([https://www.](https://www.metoc.navy.mil/jtwc/jtwc.html?cyclone)570 [metoc.navy.mil/jtwc/jtwc.html?cyclone](https://www.metoc.navy.mil/jtwc/jtwc.html?cyclone)); data for 1986 were provided from JTWC upon

571 request. Aircraft observation data during the study period are also available in the

572 Geophysical Review (No. 967 to No. 1036), which was published monthly by the JMA.

573 ERA5 data were downloaded from the Copernicus website

574 ([https://cds.climate.copernicus.eu/cdsapp#!/dataset/reanalysis-era5-single-](https://cds.climate.copernicus.eu/cdsapp#!/dataset/reanalysis-era5-single-levels?tab=overview)575 [levels?tab=overview](https://cds.climate.copernicus.eu/cdsapp#!/dataset/reanalysis-era5-single-levels?tab=overview)).

577

578

Acknowledgments

579 We thank Dr. John Knaff, Dr. Hiroyuki Yamada, Dr. Takeshi Horinouchi, Dr. Ryo Oyama,
580 Mr. Shuji Nishimura, and Mr. Yo Nyomura for their thoughtful discussions. This study was
581 supported by JST Moonshot R&D Grant Number JPMJMS2282-06 and JSPS KAKENHI
582 Grant Number 21H04992. The CI numbers and aircraft observations were provided by the
583 RSMC Tokyo and JTWC, respectively. This study was conducted for the authors' research
584 purposes and should not be regarded as an official JMA view.

586 **List of Figures**

587 Fig. 1. Number of samples used to construct a regression curve connecting the CI
588 numbers to the MSLP (reproduced from the numbers in Fig. 2a in K90). A standard
589 deviation of 12.99 hPa from the regression curve is also shown.

590

591 Fig. 2. Number of samples from Fig. 2 in K90 (red) and our count for the 12-hourly best
592 track data (blue).

593

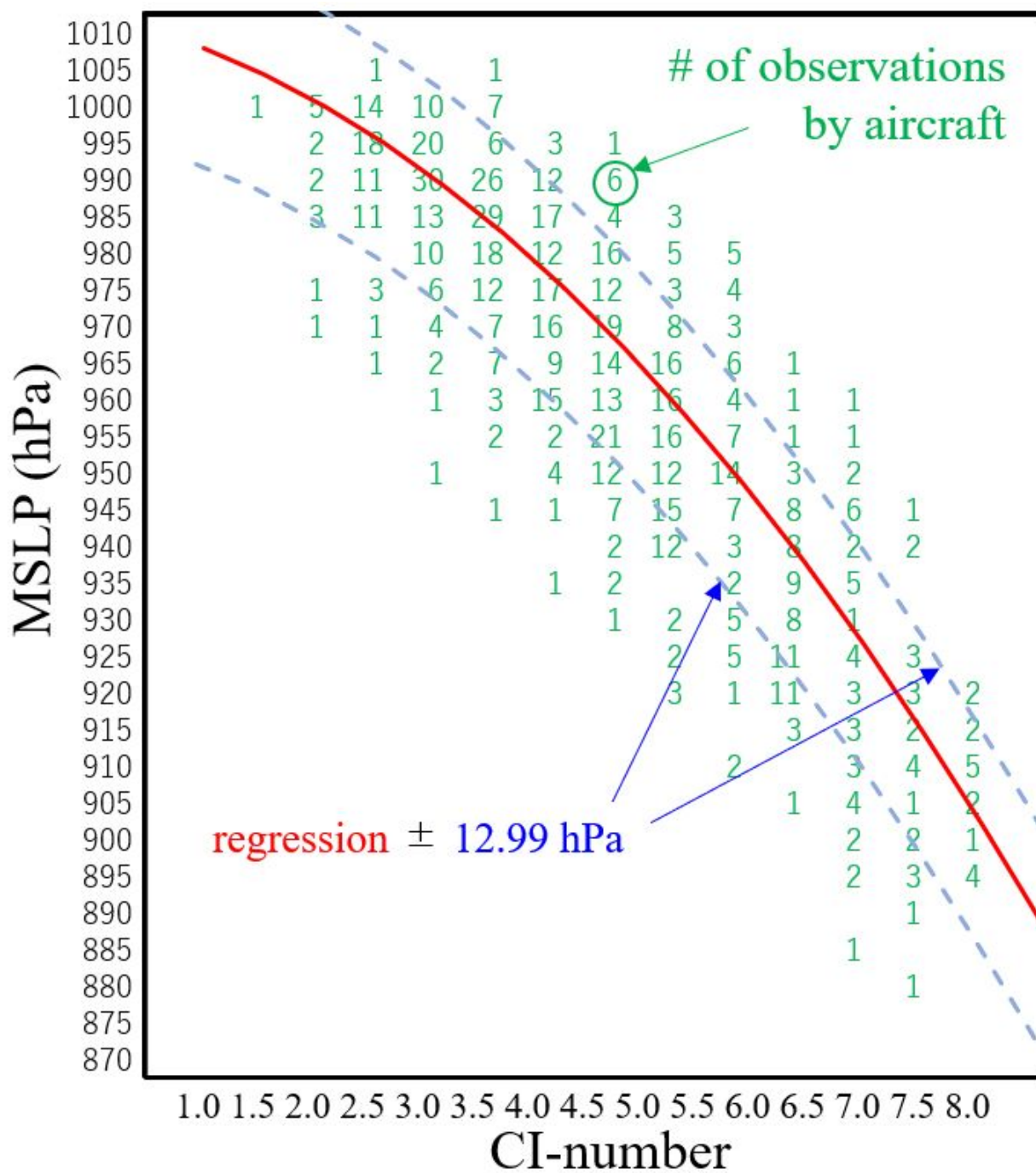
594 Fig. 3. Anomaly in the converted MSLP from aircraft altitude with respect to the
595 dropsonde-based MSLP. The conversion uses the formulae of (a) Watanabe's equation
596 and (b) Jordan's equation.

597

598 Fig. 4. Relationship between the regression models and their RMSDs.

599

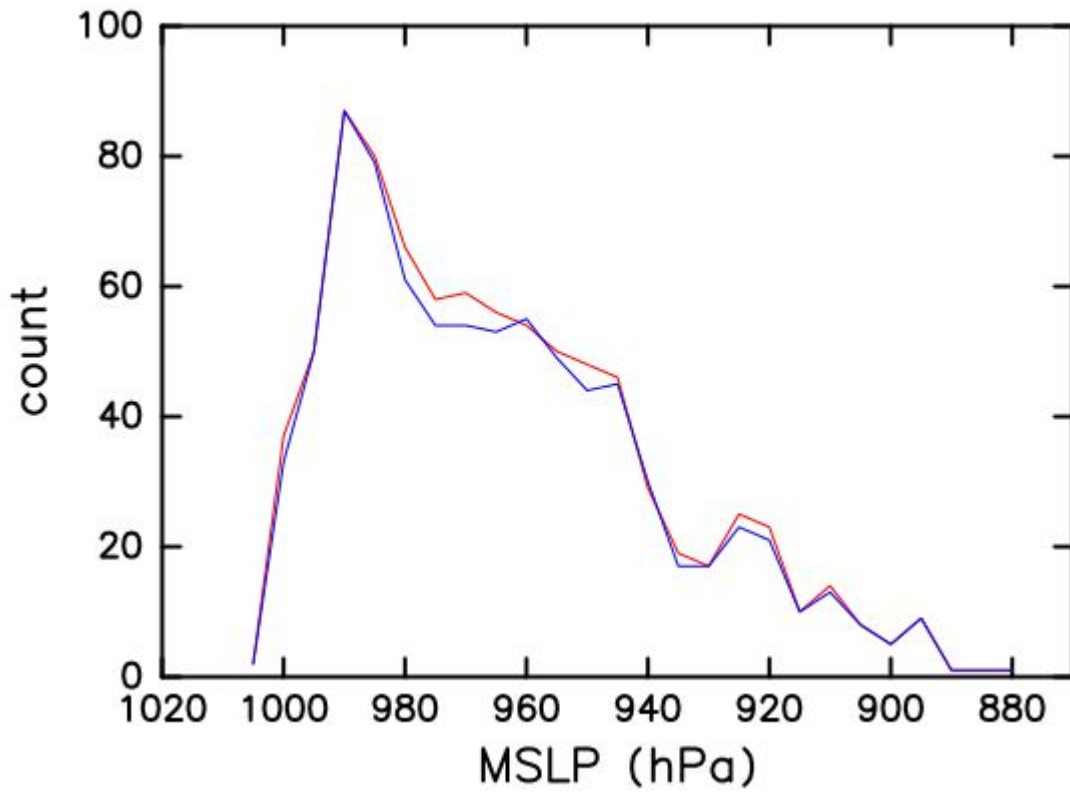
600 Fig. 5. Comparison of aircraft-based observations and regression models for CTRL and
601 TEST1.



603

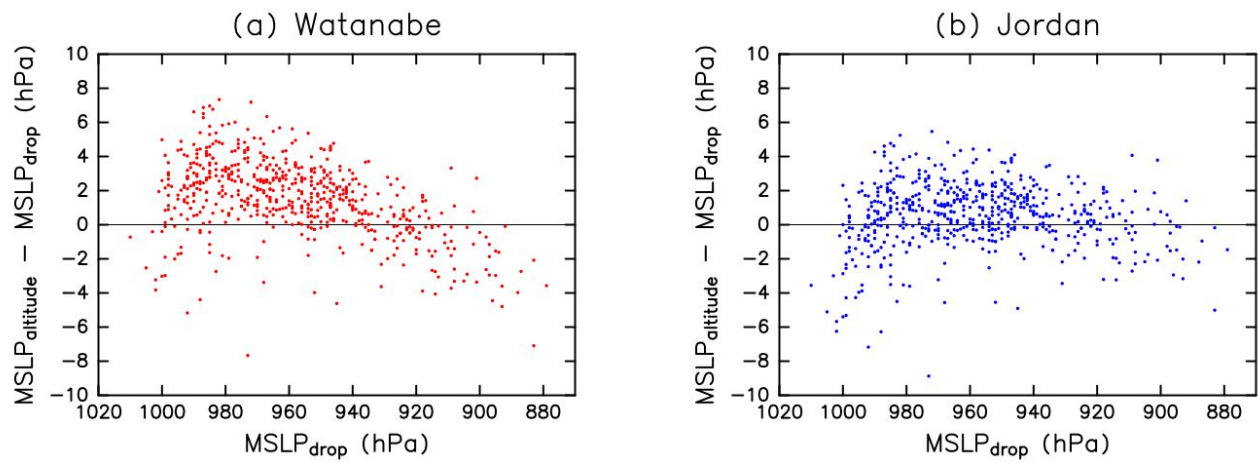
604 Fig. 1. Number of samples used to construct a regression curve connecting the CI
 605 numbers to the MSLP (reproduced from the numbers in Fig. 2a om K90). A standard
 606 deviation of 12.99 hPa from the regression curve is also shown.

608



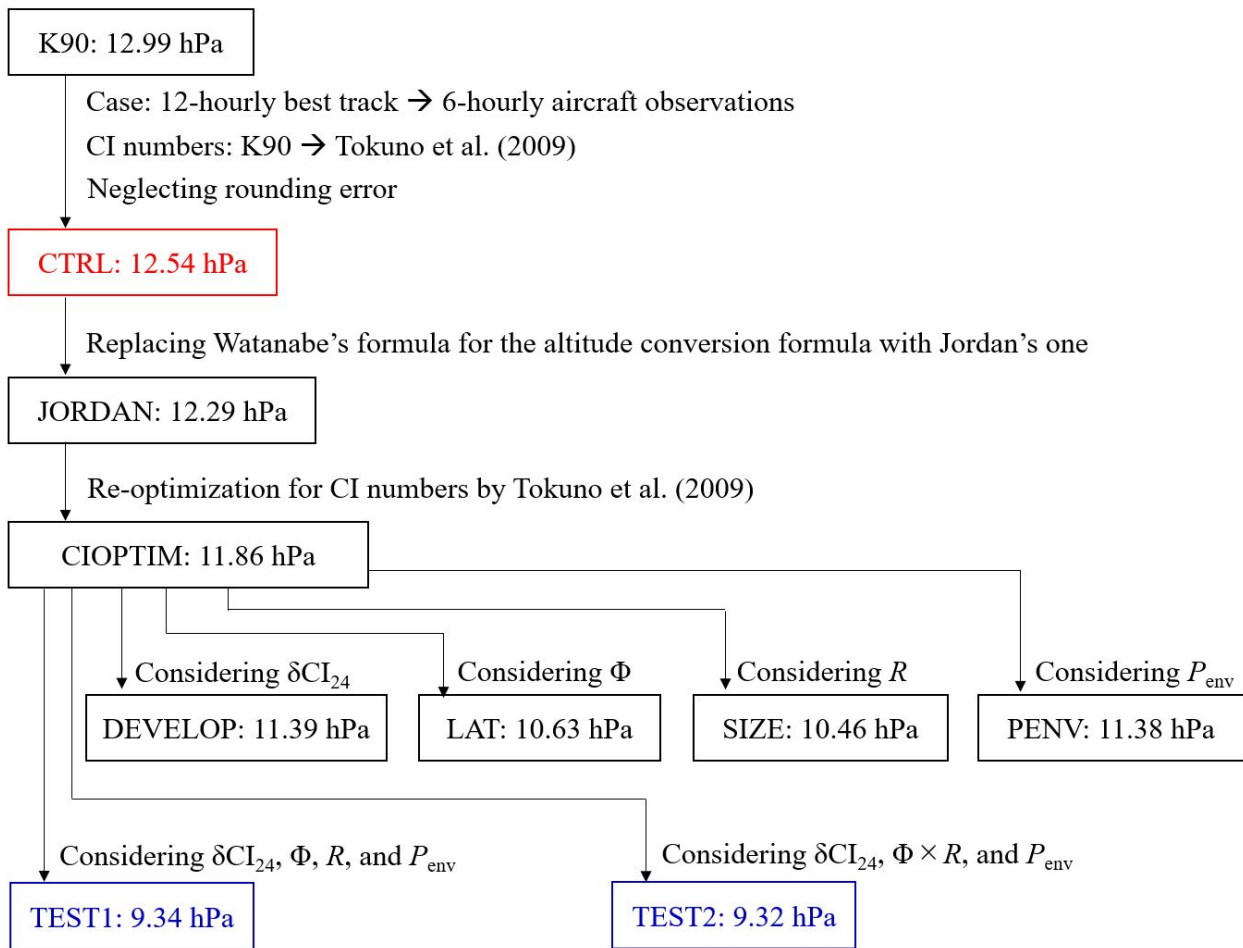
609

610 Fig. 2. Number of samples from Fig. 2 in K90 (red) and our count for the 12-hourly best
611 track data (blue).



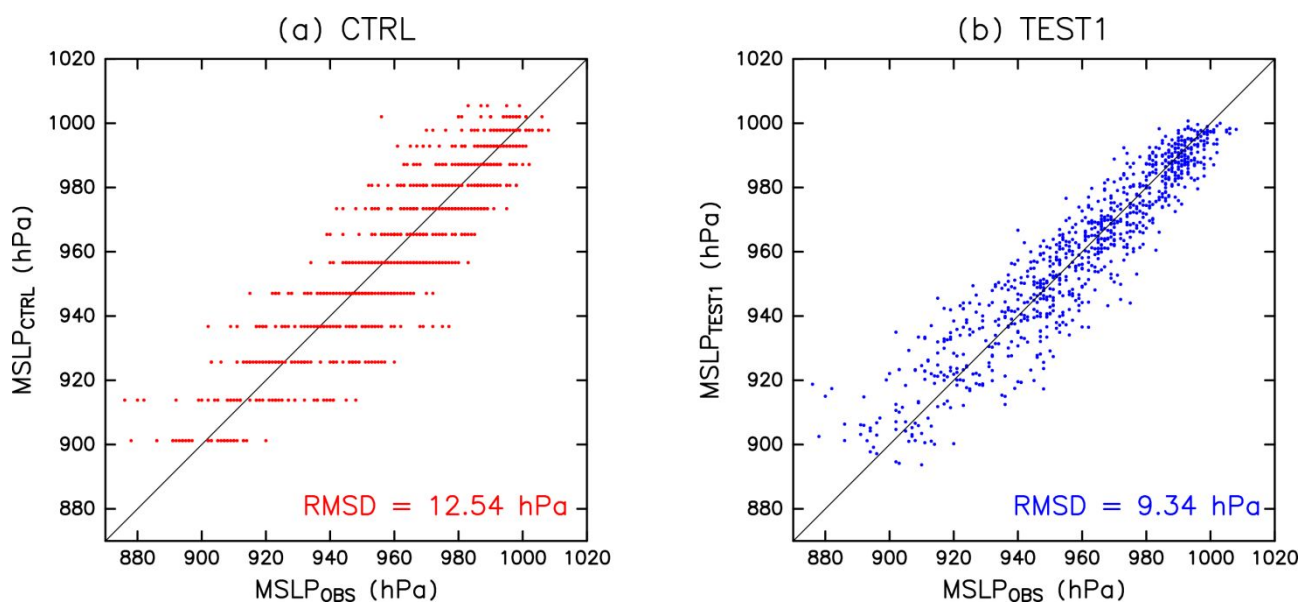
613

614 Fig. 3. Anomaly in the converted MSLP from aircraft altitude with respect to the
615 dropsonde-based MSLP. The conversion uses (a) Watanabe's equation and (b) Jordan's
616 equation.



618

619 Fig. 4. Relationship between the regression models and their RMSDs.



621

622 Fig. 5. Comparison of aircraft-based observations and regression models for CTRL and
623 TEST1.

624

625

626

627

628

629

630

631

632

633

634

635

636

637

List of Tables

638 Table 1. Regression models tested in this study. Φ is latitude in degrees and R is a size
639 parameter in km.

640

641 Table 2. Coefficients in the regression models.

642

643 Table 3. RMSD1 is the root mean squared differences between the RMSD for a model
644 outputs and reference data that are not subjected to the rounding, while $\langle \text{RMSD} \rangle$ ²
645 is the RMSD for a model with the rounding to the of aircraft-based MSLPs to the 5-hPa bin.
646 The number in the parenthesis represents the number of cases in which the deviation from
647 the aircraft-based observation is larger than 25 hPa.

648

649 Table 4. RMSDs (in hPa) in the K-fold cross validation for CTRL, JORDAN, CIOPTIM,
650 TEST1, and TEST2. The category “all” was calculated as the square root of the sum of
651 squared errors in all years.

652

653 Table 5. Experiment set to check the dependency of the skill of TEST1 on the definition of
654 size (R), environmental pressure (Penv), and dataset. The subscripts R, J, and E
655 respectively represent the data from the JMA best track, JRA55, and ERA5. An overbar
656 denotes an area average. Dataset A is the same as that used in Section 4.

657

658 Table 6. Derived equations and RMSDs of LAT, PENV, TEST1, and TEST2 for the
659 experimental set in Table 5.

660

662

Table 1. Regression models tested in this study. Φ is latitude in degrees and R is a size parameter in km.

name	equation for P_c	altitude-MSLP conversion
CTRL	$-1.53CI^2 - 3.03CI + 1010.01$	Watanabe
JORDAN	$-1.53CI^2 - 3.03CI + 1010.01$	Jordan
CIOPTIM	$a_1CI^2 + a_2CI + a_3$	Jordan
DEVELOP	$a_1CI^2 + a_2CI + a_3\delta CI_{24} + a_4$	Jordan
LAT	$a_1CI^2 + a_2CI + a_3\Phi + a_4$	Jordan
SIZE	$a_1CI^2 + a_2CI + a_3R + a_4$	Jordan
PENV	$a_1CI^2 + a_2CI + a_3 + P_{env}$	Jordan
TEST1	$a_1CI^2 + a_2CI + a_3\delta CI_{24} + a_4\Phi + a_5R + a_6 + P_{env}$	Jordan
TEST2	$a_1CI^2 + a_2CI + a_3\delta CI_{24} + a_4\Phi R + a_5 + P_{env}$	Jordan

663

664

666

Table 2. Coefficients in the regression models.

name	equation for P_c
CIOPTIM	$-1.95CI^2 + 2.64CI + 994.12$
DEVELOP	$-1.98CI^2 + 2.21CI + 2.88\delta CI_{24} + 995.91$
LAT	$-2.31CI^2 + 6.41CI - 0.911\Phi + 1001.66$
SIZE	$-1.97CI^2 + 4.09CI - 0.0282R + 999.39$
PENV	$-2.00CI^2 + 3.01CI - 14.13 + P_{env}$
TEST1	$-2.17CI^2 + 5.43CI + 1.73\delta CI_{24} - 0.367\Phi - 0.0227R - 5.78 + P_{env}$
TEST2	$-2.21CI^2 + 5.68CI + 1.39\delta CI_{24} - 0.00113\Phi R - 12.81 + P_{env}$

667

669

Table 3. RMSD is the root mean squared differences between the model outputs and reference data that are not subjected to rounding, while $\langle \text{RMSD} \rangle$ applies rounding to the MSLPs to the 5-hPa bin. The number in the parenthesis represents the number of cases in which the deviation from the aircraft-based observation is larger than 25 hPa.

name	RMSD	$\langle \text{RMSD} \rangle$
CTRL	12.54 (43)	12.62 (46)
JORDAN	12.29 (44)	12.28 (39)
CIOPTIM	11.86 (36)	11.90 (31)
DEVELOP	11.39 (20)	11.45 (19)
LAT	10.63 (30)	10.69 (22)
SIZE	10.46 (20)	10.55 (19)
PENV	11.38 (29)	11.42 (32)
TEST1	9.34 (7)	9.44 (6)
TEST2	9.32 (9)	9.43 (9)

670

672

Table 4. RMSDs (in hPa) in the K-fold cross validation for CTRL, JORDAN, CIOPTIM, TEST1, and TEST2. The category “all” was calculated as the square root of the sum of squared errors in all years.

year	1981	1982	1983	1984	1985	1986	all
CTRL	12.99	11.08	15.35	12.37	10.49	12.40	12.54
JORDAN	12.75	11.03	14.79	12.10	10.20	12.22	12.29
CIOPTIM	12.10	10.65	15.26	11.95	9.26	11.35	11.99
TEST1	10.10	7.80	11.59	10.97	8.97	8.90	9.69
TEST2	9.88	7.90	11.42	10.57	8.95	8.73	9.54
samples	119	256	139	175	47	141	877

673

675

Table 5. Experiment set to check the dependency of the skill of TEST1 on the definition of size (R), environmental pressure (P_{env}), and dataset. The subscripts R, J, and E respectively represent the data from the JMA best track, JRA55, and ERA5. An overbar denotes an area average. Dataset A is the same as that used in Section 4.

dataset	R	P_{env}
A	$R20_E$	$\overline{P_E} (R20_E+100 < r < R20_E+300)$
B	$R20_J$	$\overline{P_J} (R20_J+100 < r < R20_J+300)$
C	$R30_R$	$\overline{P_E} (R30_R+100 < r < R30_R+300)$
D	$R30_R$	$\overline{P_J} (R30_R+100 < r < R30_R+300)$
E	$R30_R$	$\overline{P_E} (R30_R+300 < r < R30_R+500)$
F	$R30_R$	$\overline{P_J} (R30_R+300 < r < R30_R+500)$
G	ROCI_E	$P_E (\text{ROCI}_E) + 1$
H	ROCI_J	$P_J (\text{ROCI}_J) + 1$

676

678

Table 6. Derived equations and RMSDs of SIZE, PENV, TEST1, and TEST2 for the experimental set in Table 5.

name	dataset	equation for P_c	RMSD
SIZE	A	$-1.97CI^2 + 4.09CI - 0.0282R + 137.74$	10.46
	B	$-1.92CI^2 + 3.74CI - 0.0359R + 137.91$	10.35
	C, D, E, F	$-2.07CI^2 + 6.17CI - 0.0437R + 132.53$	10.26
	G	$-1.89CI^2 + 2.69CI - 0.0169R + 156.95$	11.17
	H	$-1.87CI^2 + 2.45CI - 0.0190R + 157.76$	11.20
PENV	A	$-2.00CI^2 + 3.01CI - 14.12 + P_{env}$	11.38
	B	$-2.00CI^2 + 3.01CI - 14.43 + P_{env}$	11.37
	C	$-1.98CI^2 + 2.72CI - 13.15 + P_{env}$	11.19
	D	$-1.97CI^2 + 2.57CI - 12.59 + P_{env}$	11.26
	E	$-1.97CI^2 + 2.62CI - 14.33 + P_{env}$	11.36
	F	$-1.96CI^2 + 2.50CI - 14.04 + P_{env}$	11.37
	G	$-2.06CI^2 + 3.75CI - 16.39 + P_{env}$	11.23
	H	$-2.06CI^2 + 3.68CI - 16.27 + P_{env}$	11.23
TEST1	A	$-2.17CI^2 + 5.43CI + 1.73\delta CI_{24} - 0.367\Phi - 0.0227R - 5.78 + P_{env}$	9.34
	B	$-2.13CI^2 + 5.12CI + 1.65\delta CI_{24} - 0.366\Phi - 0.0279R - 1.88 + P_{env}$	9.32
	C	$-2.19CI^2 + 6.35CI + 1.38\delta CI_{24} - 0.309\Phi - 0.0317R - 6.65 + P_{env}$	9.31
	D	$-2.19CI^2 + 6.27CI + 1.38\delta CI_{24} - 0.315\Phi - 0.0323R - 5.98 + P_{env}$	9.32
	E	$-2.20CI^2 + 6.49CI + 1.37\delta CI_{24} - 0.363\Phi - 0.0320R - 7.36 + P_{env}$	9.34
	F	$-2.20CI^2 + 6.38CI + 1.38\delta CI_{24} - 0.364\Phi - 0.0320R - 7.06 + P_{env}$	9.33
	G	$-2.21CI^2 + 5.43CI + 1.79\delta CI_{24} - 0.463\Phi - 0.0153R - 3.31 + P_{env}$	9.61
	H	$-2.19CI^2 + 5.24CI + 1.76\delta CI_{24} - 0.487\Phi - 0.0173R - 0.580 + P_{env}$	9.60
TEST2	A	$-2.21CI^2 + 5.68CI + 1.39\delta CI_{24} - 0.00113\Phi R - 12.81 + P_{env}$	9.32
	B	$-2.22CI^2 + 5.67CI + 1.27\delta CI_{24} - 0.00118\Phi R - 11.46 + P_{env}$	9.37
	C	$-2.23CI^2 + 6.04CI + 1.22\delta CI_{24} - 0.00122\Phi R - 13.32 + P_{env}$	9.41
	D	$-2.22CI^2 + 5.94CI + 1.22\delta CI_{24} - 0.00124\Phi R - 12.78 + P_{env}$	9.43
	E	$-2.23CI^2 + 6.12CI + 1.22\delta CI_{24} - 0.00128\Phi R - 14.54 + P_{env}$	9.43
	F	$-2.22CI^2 + 6.00CI + 1.24\delta CI_{24} - 0.00128\Phi R - 14.25 + P_{env}$	9.43
	G	$-2.23CI^2 + 5.59CI + 1.59\delta CI_{24} - 0.000808\Phi R - 11.92 + P_{env}$	9.57
	H	$-2.23CI^2 + 5.59CI + 1.50\delta CI_{24} - 0.000845\Phi R - 11.02 + P_{env}$	9.58

679

680

681

682

684 **References**

- 685 Atkinson, G. D., and C. R. Holliday, 1977: Tropical cyclone minimum sea level
686 pressure/maximum sustained wind relationship for the western North Pacific. *Mon. Wea.*
687 *Rev.*, **105**, 421-427.
- 688 Bai, L., Y. Xu, J. Tang, and R. Guo, 2023: Interagency discrepancies in tropical cyclone
689 intensity estimates over the western North Pacific in recent years. *Atmospheric Science*
690 *Letters*, **24**, e1132.
- 691 Bai, L., H. Yu, P. G. Black, Y. Xu, M. Ying, J. Tang, and R. Guo, 2019: Reexamination of
692 the tropical cyclone wind–pressure relationship based on pre-1987 aircraft data in the
693 western North Pacific. *Wea. Fore.*, **34**, 1939-1954.
- 694 Courtney, J., and J. Knaff, 2009: Adapting the Knaff and Zehr wind-pressure relationship
695 for operational use in Tropical Cyclone Warning Centres. *Australian Meteorological and*
696 *Oceanographic Journal*, **58**, 167.
- 697 Dvorak, V. F., 1975: Tropical cyclone intensity analysis and forecasting from satellite
698 imagery. *Mon. Wea. Rev.*, **103**, 420-430.
- 699 —, 1984: *Tropical cyclone intensity analysis using satellite data*. Vol. 11, US Department
700 of Commerce, National Oceanic and Atmospheric Administration, National Environmental
701 Satellite, Data, and Information Service.
- 702 Hersbach, H., and Coauthors, 2020: The ERA5 global reanalysis. *Quart. J. Roy. Meteor.*
703 *Soc.*, **146**, 1999-2049.
- 704 Ito, K., and Coauthors, 2018: Analysis and forecast using dropsonde data from the inner-
705 core region of Tropical Cyclone Lan (2017) obtained during the first aircraft missions of T-
706 PARCII. *SOLA*, **14**, 105-110.
- 707 JMA, 1990: *Yoho-sagyo-shishin Taifu-yoho (in Japanese)*. JMA, 150 pp.
- 708 Jordan, C., 1958: Estimation of surface central pressures in tropical cyclones from aircraft
709 observations. *Bull. Amer. Meteor. Soc.*, **39**, 345-352.
- 710 Kawabata, Y., U. Shimada, and M. Yamaguchi, 2023: The 30-year (1987-2016) Trend of
711 Strong Typhoons and Genesis Locations Found in the Japan Meteorological Agency's
712 Dvorak Reanalysis Data. *J. Meteor. Soc. Japan*.
- 713 Kitabatake, N., K. Kato, and M. Tokuno, 2018: Reexamination of the Relationship between
714 Central Pressure of Tropical Cyclones in the Western North Pacific and CI Numbers of the
715 Dvorak's technique using aircraft reconnaissance in the 1980s (in Japanese). *Journal of*
716 *Meteorological Research*, **67**, 1-20.
- 717 Knaff, J. A., and R. M. Zehr, 2007: Reexamination of tropical cyclone wind–pressure
718 relationships. *Wea. Fore.*, **22**, 71-88.
- 719 Koba, H., T. Hagiwara, S. Osano, and S. Akashi, 1990: Relationships between CI Number
720 from Dvorak's technique and minimum sea level pressure or maximum wind speed of
721 tropical cyclone. *J. Meteor. Res.*, **42**, 59-67.
- 722 —, 1991a: Relationships between CI Number and minimum sea level pressure/maximum
723 wind speed of tropical cyclones. *Geophysical Magazine*, **44**, 15-25.

- 724 Koba, H., S. Osano, T. Hagiwara, S. Akashi, and T. Kikuchi, 1991b: A New Rule of CI
725 Number Determination in the Dvorak Technique for Tropical Cyclones Crossing the
726 Philippine Islands. *The Geophysical Magazine*, **44**, 7.
- 727 Kobayashi, S., and Coauthors, 2015: The JRA-55 reanalysis: General specifications and
728 basic characteristics. *Journal of the Meteorological Society of Japan. Ser. II*, **93**, 5-48.
- 729 Lushine, J. B., 1977: A relationship between weakening of tropical cyclone cloud patterns
730 and lessening of wind speed. *NOAA technical memorandum*, **85**, 12pp.
- 731 Nakazawa, T., and S. Hoshino, 2009: Intercomparison of Dvorak parameters in the tropical
732 cyclone datasets over the western North Pacific. *SOLA*, **5**, 33-36.
- 733 Olander, T. L., and C. S. Velden, 2019: The advanced Dvorak technique (ADT) for
734 estimating tropical cyclone intensity: Update and new capabilities. *Wea. Fore.*, **34**, 905-922.
- 735 Oyama, R., 2014: Algorithm and validation of a tropical cyclone central pressure
736 estimation method based on warm core intensity as observed using the Advanced
737 Microwave Sounding Unit-A (AMSU-A). *RSMC Tokyo Technical Review*, **16**.
- 738 Shimada, U., M. Sawada, and H. Yamada, 2016: Evaluation of the accuracy and utility of
739 tropical cyclone intensity estimation using single ground-based Doppler radar observations.
740 *Mon. Wea. Rev.*, **144**, 1823-1840.
- 741 Takahashi, K., 1952: Techniques of the typhoon forecast. *Geophysical Magazine*, **24**, 1-8.
- 742 Tokuno, M., S. Yoshida, A. Shouji, M. Sakai, and M. Hirohata, 2009: Relationship among
743 reanalyzed typhoon CI numbers, minimum sea level pressure, and maximum wind speed
744 (in Japanese). *Fall meeting of Meteorological Society of Japan*, Fukuoka, Meteorological
745 Society of Japan.
- 746 Velden, C., and Coauthors, 2006: The Dvorak tropical cyclone intensity estimation
747 technique: A satellite-based method that has endured for over 30 years. *Bull. Amer.*
748 *Meteor. Soc.*, **87**, 1195-1210.
- 749 Yamada, H., and Coauthors, 2021: The double warm-core structure of Typhoon Lan
750 (2017) as observed through the first Japanese eyewall-penetrating aircraft reconnaissance.
751 *Journal of the Meteorological Society of Japan. Ser. II*, **99**, 1297-1327.
- 752 Zhang, B., W. Perrie, J. A. Zhang, E. W. Uhlhorn, and Y. He, 2014: High-resolution
753 hurricane vector winds from C-band dual-polarization SAR observations. *Journal of*
754 *Atmospheric and Oceanic Technology*, **31**, 272-286.

755

756